Mechanistic Study on the Insertion of Phenylacetylene into *cis*-Bis(silyl)platinum(II) Complexes

Fumiyuki Ozawa* and Jun Kamite

Department of Applied Chemistry, Faculty of Engineering, Osaka City University, Sumiyoshi-ku, Osaka 558-8585, Japan

Received July 20, 1998

Four bis(silyl)platinum complexes *cis*-Pt(SiR_3)$_2$(PMe_2Ph)$_2$ (SiR_3 = $SiMe_2Ph$ (**1a**), $SiMePh_2$ (**1b**), $SiPh_3$ (**1c**), $SiFPh_2$ (**1d**)) have been prepared and their reactions with alkynes and alkenes examined. The X-ray structures of **1a**−**c** exhibit significant distortion from the square planar geometry in the order **1b** > **1c** > **1a**. Complexes **1a**−**d** react with phenylacetylene in solution to give the corresponding insertion complexes *cis*-Pt{C(Ph)=CH(SiR_3)}(SiR_3)(PMe_2-Ph)$_2$ (**2a**−**d**). Complex **1c** reacts also with acetylene to afford the insertion complex *cis*-Pt-(CH=CH$SiPh_3$)($SiPh_3$)(PMe_2Ph)$_2$ (**2e**), whose structure has been determined by X-ray diffraction study. Kinetic studies indicate the insertion process involving prior dissociation of PMe_2Ph ligand from **1**, followed by insertion of phenylacetylene into the Pt−SiR_3 bond. The reactivity toward insertion decreases in the order **1c** > **1a** > **1b** ≫ **1d**. Factors responsible for the reactivity order are discussed on the basis of kinetic data and X-ray structures.

Introduction

Bis-silylation of unsaturated hydrocarbons catalyzed by group 10 metals is a useful means of synthesizing organosilicon compounds, in which two Si−C bonds are created in one reaction.[1] This reaction is generally assumed to proceed via sequence of the following elementary processes.[2] The first step is oxidative addition of disilane to a low-valent metal species to give a bis(silyl) complex.[3] Insertion of a carbon−carbon multiple bond into the resulting metal−silicon bond provides an organo(silyl)metal intermediate,[4−6] which reductively eliminates bis-silylation product.[7,8] Although these elementary processes have been documented with isolated silyl complexes,[2−8] the factors governing the reactivity, particularly for the insertion and reductive elimination processes, have remained to be explored.[9]

In this study we examined structures and insertion reactions with alkynes and alkenes of a series of bis-(silyl)platinum complexes, *cis*-Pt(SiR_3)$_2$(PMe_2Ph)$_2$ (SiR_3 = $SiMe_2Ph$ (**1a**), $SiMePh_2$ (**1b**), $SiPh_3$ (**1c**), $SiFPh_2$ (**1d**)). Tanaka and co-workers previously reported that *cis*-Pt-($SiMe_2Ph$)$_2$($PMePh_2$)$_2$ reacts with a variety of alkynes and alkenes to give bis-silylation products,[4] where no insertion complexes were detected. On the other hand, the present bis(silyl) complexes coordinated with PMe_2-Ph ligands have been found to provide the insertion complexes of phenylacetylene *cis*-Pt{C(Ph)=CH-(SiR_3)}(SiR_3)(PMe_2Ph)$_2$, which can be isolated. Thus we could carry out detailed investigations into the insertion mechanism using kinetic techniques and X-ray structural analyses. We herein show an interesting relation between the reactivities and the structures of bis(silyl) complexes that hitherto has not been observed.

(1) For recent examples see: Tsuji, Y.; Funato, M.; Ozawa, M.; Ogiyama, H.; Kajita, S.; Kawamura, T. *J. Org. Chem.* **1996**, *61*, 5779. Obara, Y. Tsuji, Y. Kawamura, T. *Organometallics* **1993**, *12*, 2853; *J. Am. Chem. Soc.* **1993**, *115*, 10414; *J. Am. Chem. Soc.* **1995**, *117*, 9814. Murakami, M.; Oike, H.; Sugawara, M.; Suginome, M.; Ito, Y. *Tetrahedron* **1993**, *49*, 3933. Murakami, M.; Suginome, M.; Fujimoto, K.; Nakamura, H.; Andersson, P. G.; Ito, Y. *J. Am. Chem. Soc.* **1993**, *115*, 6487. Finckh, W.; Tang, B.; Lough, A.; Manners, I. *Organometallics* **1992**, *11*, 2904. Tsuji, Y.; Lago, R. M.; Tomohiro, S.; Tsuneishi, H. *Organometallics* **1992**, *11*, 2353. Yamashita, H.; Catellani, M.; Tanaka, M. *Chem. Lett.* **1991**, 241. Ito, Y.; Suginome, M.; Murakami, M. *J. Org. Chem.* **1991**, *56*, 1948. Murakami, M.; Andersson, P. G.; Suginome, M.; Ito, Y. *J. Am. Chem. Soc.* **1991**, *113*, 3987. Kusumoto, T.; Hiyama, T. *Bull. Chem. Soc. Jpn.* **1990**, *63*, 3103. Hayashi, T.; Kobayashi, T.; Kawamoto, A. M.; Yamashita, H.; Tanaka, M. *Organometallics* **1990**, *9*, 280. Hayashi, T.; Kawamoto, A. M.; Kobayashi, T.; Tanaka, M. *J. Chem. Soc., Chem. Commun.* **1990**, 563. For further references see: Ozawa, F.; Sugawara, M.; Hayashi, T. *Organometallics* **1994**, *13*, 3237.

(2) Brunstein, P.; Knorr, M. *J. Organomet. Chem.* **1995**, *500*, 21. Recatto, C. A. *Aldrichimica Acta* **1995**, *28*, 85.

(3) Yamashita, H.; Kobayashi, T.; Hayashi, T.; Tanaka, M. *Chem. Lett.* **1990**, 1447. Murakami, M.; Yoshida, T.; Ito, Y. *Organometallics* **1994**, *13*, 2900. Suginome, M.; Oike, H.; Park, S.-S.; Ito, Y. *Bull. Chem. Soc. Jpn.* **1996**, *69*, 289. Suginome, M.; Oike, H.; Shuff, P. H.; Ito, Y. *Organometallics* **1996**, *15*, 2170.

(4) Kobayashi, T.; Hayashi, T.; Yamashita, H.; Tanaka, M. *Chem. Lett.* **1989**, 467.

(5) Chatt, J.; Eaborn, C.; Kapoor, P. N. *J. Organomet. Chem.* **1970**, *23*, 109. Kiso, Y.; Tamao, K.; Kumada, M. *J. Organomet. Chem.* **1974**, *76*, 105. Eaborn, C.; Metham, T. N.; Pidcock, A. *J. Organomet. Chem.* **1977**, *131*, 377. Seyferth, D.; Goldman, E. W.; Escudié, J. *J. Organomet. Chem.* **1984**, *271*, 337. Tanaka, M.; Uchimaru, Y.; Lautenschlager, H. J. *Organometallics* **1991**, *10*, 16. Pan, Y.; Mague, J. T.; Fink, M. J. *Organometallics* **1992**, *11*, 3495. Yamashita, H.; Tanaka, M.; Goto, M. *Organometallics* **1993**, *12*, 988.

(6) Ozawa, F.; Hikida, T. *Organometallics* **1996**, *15*, 4501.

(7) Tanaka, Y.; Yamashita, H.; Shimada, S.; Tanaka, M. *Organometallics* **1997**, *16*, 3246.

(8) Ozawa, F.; Hikida, T.; Hayashi, T. *J. Am. Chem. Soc.* **1994**, *116*, 2844. Ozawa, F.; Hikida, T.; Hasebe, K.; Mori, T. *Organometallics* **1998**, *17*, 1018.

(9) For theoretical studies see: (a) Sakaki, S.; Mizoe, N.; Sugimoto, M. *Organometallics* **1998**, *17*, 2510. (b) Sakaki, S.; Ogawa, M.; Musashi, Y. *J. Organomet. Chem.* **1997**, *535*, 25. (c) Sakaki, S.; Mizoe, N.; Sumi, N.; Biswas, B.; Sugimoto, M. *Abstracts of 44th Symposium on Organometallic Chemistry*, Japan; Kinki Chemical Society: Osaka, Japan, 1997; PA 105. (d) Sakaki, S.; Ogawa, M.; Kinoshita, M. *J. Phys. Chem.* **1995**, *99*, 9933. (e) Sakaki, S.; Ogawa, M.; Musashi, Y.; Arai, T. *J. Am. Chem. Soc.* **1994**, *116*, 7258. (f) Hada, M.; Tanaka, Y.; Ito, M.; Murakami, M.; Amii, H.; Ito, Y.; Nakatsuji, H. *J. Am. Chem. Soc.* **1994**, *116*, 8754.

10.1021/om980610w CCC: $15.00
Publication on Web 11/20/1998

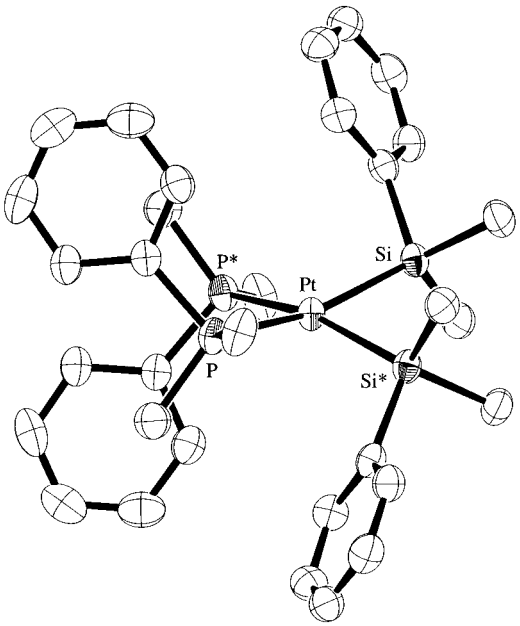

Figure 1. Molecular structure of *cis*-$Pt(SiMe_2Ph)_2(PMe_2Ph)_2$ (**1a**). Thermal ellipsoids are drawn at the 30% probability level.

Results

Preparation and X-ray Structures of *cis*-Bis(silyl)platinum(II) Complexes. Complexes **1a** and **1b** were synthesized by the reactions of *cis*-$PtCl_2(PMe_2Ph)_2$ with (organosilyl)lithium (2.2 equiv) in tetrahydrofuran (THF).[10] Since the yield of **1c** prepared by the same method was rather low (13%), this complex was synthesized in 93% yield by the following route. Treatment of *trans*-$PtCl(SiPh_3)(PMe_2Ph)_2$ [10] with $LiSiPh_3$ in THF at −50 °C provided *trans*-$Pt(SiPh_3)_2(PMe_2Ph)_2$ ($^{31}P\{^1H\}$ NMR: δ −11.7, $^1J_{Pt-P}$ = 2700 Hz), which quickly isomerized to **1c** at room temperature. Complex **1d** was prepared by the reaction of *cis*-$PtMe(SiPh_3)(PMe_2Ph)_2$[6] with $HSiFPh_2$ (10 equiv) in benzene. All complexes thus prepared were characterized by NMR spectroscopy and elemental analysis. Complexes **1a** and **1c** were identified also by X-ray diffraction studies (Figures 1 and 2).

The structural parameters and $^{31}P\{^1H\}$ NMR data for **1a**−**c** are summarized in Table 1. The data for **1b** are quoted from a recent report by Tsuji and co-workers.[11a] Also included in this table are structural parameters for *cis*-$Pt(SiH_3)_2(PH_3)_2$ (**1e**), which were estimated by Sakaki and co-workers using ab initio MO calculation.[9d] Tolman's cone angles (θ)[12] are given for indexes of bulkiness of silyl ligands.[13]

As already documented for **1b**,[11a] bis(triorganosilyl)platinum complexes including **1a** and **1c** have twisted square planar geometry around platinum distinctly distorted from planarity.[14] Since **1e** bearing compact SiH_3 and PH_3 ligands has no distortion, the structural variation observed for **1a**−**c** may be attributed primarily to the difference in bulkiness of silyl ligands. Actually, the Si−Pt−Si angles and the distances between the two silicon atoms (Si···Si) are significantly larger than those of **1e** and increase with increasing bulkiness of silyl ligands (**1a** < **1b** < **1c**). On the other hand, dihedral angles between the PtP_2 and the $PtSi_2$ plane exhibit irregularity in their order (**1a** < **1c** < **1b**), not simply accounted for by steric congestion around platinum. Thus **1b** with $SiMePh_2$ ligands in the middle size has the most twisted structure, while **1c** with the biggest

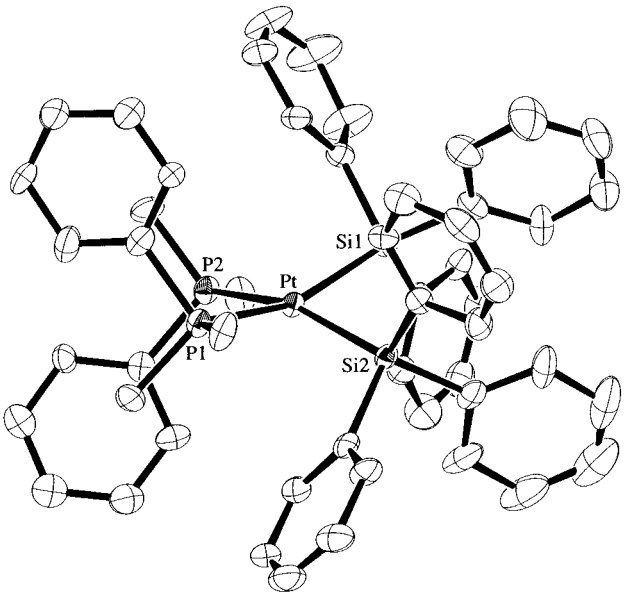

Figure 2. Molecular structure of *cis*-$Pt(SiPh_3)_2(PMe_2Ph)_2$ (**1c**). Thermal ellipsoids are drawn at the 30% probability level.

Table 1. Selected Bond Distances and Angles and $^{31}P\{^1H\}$ NMR Data for 1a−c

complex	**1a**	**1b**[a]	**1c**	**1e**[b]
SiR_3	$SiMe_2Ph$	$SiMePh_2$	$SiPh_3$	SiH_3
θ[c] (deg)	122	136	145	87
		Distances (Å)		
Pt−Si	2.370(1)	2.359(2)	2.374(3) 2.373(3)	2.371
Pt−P	2.3701(9)	2.352(2)	2.396(2) 2.408(3)	2.464
Si···Si	3.233(1)	3.304(4)	3.334(4)	3.111
		Angles (deg)		
Si−Pt−Si	86.02(5)	88.91(9)	89.22(9)	82.0
P−Pt−P	93.63(5)	96.48(10)	93.49(9)	97.0
Si−Pt−P	163.52(4)	152.42(7)	159.5(1) 159.7(1)	172.0
DA[d]	22.80	38.1	28.34	0.0
		$^{31}P\{^1H\}$ NMR Data[e]		
δ	−6.6	−7.6	−10.2	
$^1J_{Pt-P}$ (Hz)	1528 (1542)	1560 (1572)	1508 (1536)	
T_c (°C) [f]	−35	−10	0	

[a] The data taken from ref 11a. [b] Theoretical values for *cis*-$Pt(SiH_3)_2(PH_3)_2$ taken from ref 9d. [c] Tolman's cone angles for the corresponding phosphine ligands (see text). [d] Dihedral angles between PtP_2 and $PtSi_2$ planes. [e] The data at 23 °C. $^1J_{Pt-P}$ constants in parentheses are the values measured at −70 °C. [f] Coalescence temperature for the satellite signals due to P−Si(transoid) and P−Si(cisoid) couplings (see text).

(10) Chatt, J.; Eaborn, C.; Ibekwe, S. D.; Kapoor, P. N. *J. Chem. Soc. A* **1970**, 1343.
(11) (a) Tsuji, Y.; Nishiyama, K.; Hori, S.; Ebihara, M.; Kawamura, T. *Organometallics* **1998**, *17*, 507. (b) Obora, Y.; Tsuji, Y.; Nishiyama, Y.; Ebihara, M.; Kawamura, T. *J. Am. Chem. Soc.* **1996**, *118*, 10922.
(12) Tolman, C. A. *Chem. Rev.* **1977**, *77*, 313.
(13) Covalent radii of silicon and phosphorus are almost identical with each other.
(14) Similar distortion from square planar geometry has been observed for X-ray structures of bis(germyl)[15] and bis(stannyl)[11] complexes.
(15) Yamashita, H.; Kobayashi, T.-a.; Tanaka, M. *Organometallics* **1992**, *11*, 2330. Hatanaka, W.; Wada, T.; Mochida, K.; Yamamoto, A. *Abstracts of 45th Symposium on Organometallic Chemistry, Japan*; Kinki Chemical Society: Tokyo, Japan, 1998; PA 137.

$SiPh_3$ ligands shows the medium dihedral angle. It is further noted that **1b** with the most twisted structure has the shortest Pt−Si and Pt−P bonds. Since bond lengths between metal center and coordinated atoms in square planar complexes are known to vary with trans influence,[16] the significant distortion in **1b**, which reduces the direct labilizing interaction between mutually trans ligands, may be responsible for the shortest bonds.

Tsuji and co-workers have recently demonstrated that bis(silyl)- and bis(stannyl)platinum complexes including **1b** undergo a rapid twist-rotation via a pseudo tetrahedral transition state in solution, which may be confirmed by coalescence phenomena between satellite signals due to P−E(transoid) and P−E(cisoid) couplings (E = Si, Sn) in $^{31}P\{^1H\}$ NMR spectra.[11] In this study we observed similar fluxional behavior for **1a** and **1c**. As judging from the coalescence temperatures (T_c) listed in Table 1, the ease of twist-rotation decreases in the other **1a** > **1b** > **1c**, probably reflecting increasing electron-withdrawing character of silyl ligands in this order.[11b]

Despite the occurrence of a rapid twist-rotation in solution, however, the $^1J_{Pt-P}$ values observed in $^{31}P\{^1H\}$ NMR spectra are nicely correlated with the Pt−P bond lengths determined by X-ray structural analysis (Table 1). Thus the $^1J_{Pt-P}$ constants increase as the Pt−P distances in the crystals decrease (**1c** > **1a** > **1b**). Especially, complex **1b**, which has distinctly shorter Pt−P bonds than the others, exhibits a significantly larger $^1J_{Pt-P}$ value at ambient (23 °C) as well as at low temperature (−70 °C). Therefore, we may consider that the structural features observed in the crystals are preserved in solution as well.

Reactions with Alkynes and Alkenes. Complexes **1a**−**c** instantly reacted with phenylacetylene (1 equiv) at room temperature in CH_2Cl_2 to give the corresponding insertion complexes **2a**−**c** in quantitative yields as confirmed by $^{31}P\{^1H\}$ NMR spectroscopy (eq 1). Complex **1d** was much less reactive, but underwent the insertion of 1 equiv of phenylacetylene within 10 min at 60 °C in benzene in the presence of an excess amount of phenylacetylene (5 equiv).

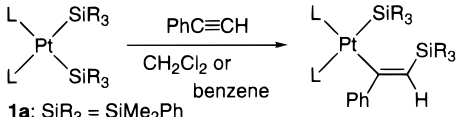

1a: $SiR_3 = SiMe_2Ph$
1b: $SiR_3 = SiMePh_2$
1c: $SiR_3 = SiPh_3$
1d: $SiR_3 = SiFPh_2$ L = PMe_2Ph

(1)

Complexes **2a**−**d** were isolated as white solids and characterized by NMR spectroscopy and elemental analysis. The occurrence of regioselective insertion of phenylacetylene, leading to the form of *cis*-Pt{C(Ph)=CH(SiR_3)}(SiR_3)(PMe_2Ph)$_2$, was confirmed by comparison of the NMR data of **2a**−**d** with those of *cis*-PtMe{C(Ph)=CH($SiPh_3$)}(PMe_2Ph)$_2$, whose structure was previously determined by X-ray analysis.[6] For example, the β-hydrogen of the alkenyl ligand in **2a** appeared at δ 7.66 (dd) with large and small couplings to trans and cis phosphorus nuclei ($^4J_{P-H}$ = 19.5 and 3.9 Hz); the coupling constants are consistent with the *Z* arrangement around the C=C double bond. The α- and β-olefinic carbons were observed at δ 182.9 (dd, $^2J_{P-C}$ = 100 and 16 Hz) and 125.8 (s), respectively. The absence of hydrogen at the α-carbon and the presence at the β-carbon were confirmed by ^{13}C NMR spectroscopy in a DEPT mode. Complexes **2b**−**d** showed comparable NMR data (see Experimental Section).

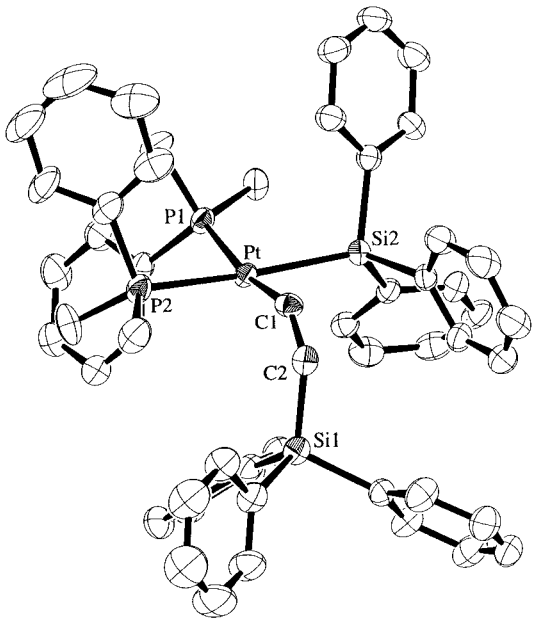

Figure 3. Molecular structure of *cis*-Pt(CH=CH$SiPh_3$)($SiPh_3$)(PMe_2Ph)$_2$ (**2e**). Thermal ellipsoids are drawn at the 30% probability level. Selected bond distances (Å) and angles (deg): Pt−C1 = 2.043(6), C1−C2 = 1.338(8), C2−Si1 = 1.844(7), Pt−Si2 = 2.389(2), Pt−P1 = 2.330(2), Pt−P2 = 2.366(2), Pt−C1−C2 = 139.7(5), C1−C2−Si1 = 132.9(5), C1−Pt−Si2 = 83.5(2), C1−Pt−P2 = 88.6(2), P1−Pt−Si2 = 92.52(5), P1−Pt−P2 = 93.96(6), C1−Pt−P1 = 169.4(2), P2−Pt−Si2 = 169.49(6).

Several alkynes and alkenes were also employed for the reactions with **1c**, which possesses the highest reactivity (vide infra). Dimethyl acetylenedicarboxylate was inactive toward insertion at room temperature and led to rapid decomposition of **1c**, giving $Ph_3SiSiPh_3$. Diphenylacetylene, 3-hexyne, *tert*-butylacetylene, and styrene were also unreactive with **1c**. On the other hand, ethylene, acetylene, and 1-hexyne exhibited insertion reactivity. The reaction with an excess amount of ethylene proceeded at room temperature to give CH_2=CH$SiPh_3$ in 93% yield (GLC). The reaction with acetylene at 0 °C provided the insertion complex *cis*-Pt(CH=CH$SiPh_3$)($SiPh_3$)(PMe_2Ph)$_2$ (**2e**), which was isolated in 86% yield. The formation of insertion complex was also noted with 1-hexyne (3 equiv), but its isolation was unsuccessful due to decomposition.

Figure 3 shows the X-ray structure of **2e**. The platinum atom is in a slightly distorted square planar environment; the sum of four angles about platinum is 358.6°. The C1−C2 distance (1.338(8) Å) is in the typical range of a carbon−carbon double bond. The Pt−C1−C2 and C1−C2−Si1 angles (139.7(5) and 132.9(5)°, respectively) are considerably wider than typical sp^2 carbons, probably due to steric reasons. The cis ar-

(16) Appleton, T. G.; Clark, H. C.; Manzer, L. E. *Coord. Chem. Rev.* **1973**, *10*, 335. Bresciani-Pahor, N.; Forcolin, M.; Marzilli, L. G.; Randaccio, L.; Summers, M. F.; Toscano, P. J. *Coord. Chem. Rev.* **1985**, *63*, 1.

Table 2. Pseudo-First-Order Rate Constants and Kinetic Parameters for the Insertion of Phenylacetylene into Bis(silyl) Complexes 1a−d[a]

1a (at −5 °C)	$k_{obsd} = 1.15 \times 10^{-4}$ s^{-1}	$\Delta G^{\ddagger} = 20.5$ kcal mol^{-1}
	$\Delta H^{\ddagger} = 25.4(4)$ kcal mol^{-1}	$\Delta S^{\ddagger} = 18.4(2)$ eu
1b (at −5 °C)	$k_{obsd} = 4.11 \times 10^{-5}$ s^{-1}	$\Delta G^{\ddagger} = 21.0$ kcal mol^{-1}
	$\Delta H^{\ddagger} = 29.8(4)$ kcal mol^{-1}	$\Delta S^{\ddagger} = 32.9(2)$ eu
1c (at −5 °C)[b]	$k_{obsd} = 1.18 \times 10^{-3}$ s^{-1}	$\Delta G^{\ddagger} = 19.2$ kcal mol^{-1}
	$\Delta H^{\ddagger} = 26.6(9)$ kcal mol^{-1}	$\Delta S^{\ddagger} = 27.5(3)$ eu
1d (at +50 °C)	$k_{obsd} = 8.08 \times 10^{-4}$ s^{-1}	

[a] All kinetic runs were conducted in CD_2Cl_2 except for **1d** ($CDCl_3$). Initial concentration: [complex] = 20−25 mM, [PhC≡CH] = 0.50 M. The activation parameters were estimated from Eyring plots in the temperature range: −10 to +5 °C for **1a** ($r = 0.999$), −5 to +10 °C for **1b** ($r = 1.00$), −25 to −10 °C for **1c** ($r = 0.999$). [b] The rate constant at −5 °C was extrapolated from the Eyring plot.

rangement of the platinum and silicon atoms around the C=C double bond clearly shows the occurrence of cis insertion of acetylene into the Pt−Si bond.

Kinetic Study on the Insertion of Phenylacetylene. Time courses of the reactions of **1a**−**d** with phenylacetylene in CD_2Cl_2 (for **1a**−**c**) or $CDCl_3$ (for **1d**) were followed by NMR spectroscopy. In the presence of an excess amount of phenylacetylene (>10 equiv), all reactions obeyed first-order kinetics with respect to the concentration of starting complexes over 70% conversion. Table 2 lists the rate constants together with the activation parameters for **1a**−**c**, showing the following reactivity order: **1c** > **1a** > **1b** ≫ **1d**. The lowest reactivity of **1d** is probably due to the strongest Pt−$SiFPh_2$ bond; the M−Si bond energy is known to increase with increasing electron affinity of the silyl ligand, which is enhanced by electron-withdrawing substituents at silicon.[9c] On the other hand, the reactivity order observed for **1a**−**c** are apparently inconsistent with the electronic nature of silyl ligands. To examine the reason for this irregularity, we next carried out detailed kinetic experiments on the insertion mechanism.

Dependence of the reaction rate of **1b** on the concentration of PMe_2Ph and PhC≡CH added to the system is shown in Figures 4 and 5, respectively. The reaction progress was retarded by addition of free PMe_2Ph to the system; reciprocals of the rate constants were linearly correlated with the concentration of PMe_2Ph added to the system ($r = 0.989$; Figure 4). Furthermore, a good linear correlation was observed between the $1/k_{obsd}$ and 1/[PhC≡CH] values ($r = 1.00$; Figure 5).[17]

These kinetic observations are consistent with the insertion mechanism depicted in Scheme 1 (SiR_3 = $SiMePh_2$). The first step is dissociation of one of the PMe_2Ph ligands (L) from **1b** to give the three-coordinate bis(silyl) intermediate **3b**, which successively undergoes migratory insertion of phenylacetylene into the Pt−$SiMePh_2$ bond via prior coordination of phenylacetylene to the vacant site of **3b**. The resulting **4b** is then rapidly converted to the final product **2b** by trans to cis isomerization followed by coordination of PMe_2Ph liberated in the system.

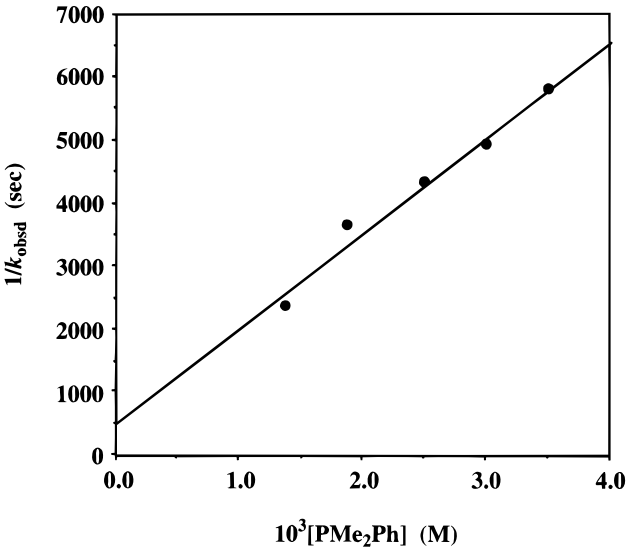

Figure 4. Effect of added PMe_2Ph on the insertion rate of phenylacetylene into **1b** in CD_2Cl_2 at −5 °C. Initial concentration: [**1b**] = 0.025 M; [PhC≡CH] = 0.25 M.

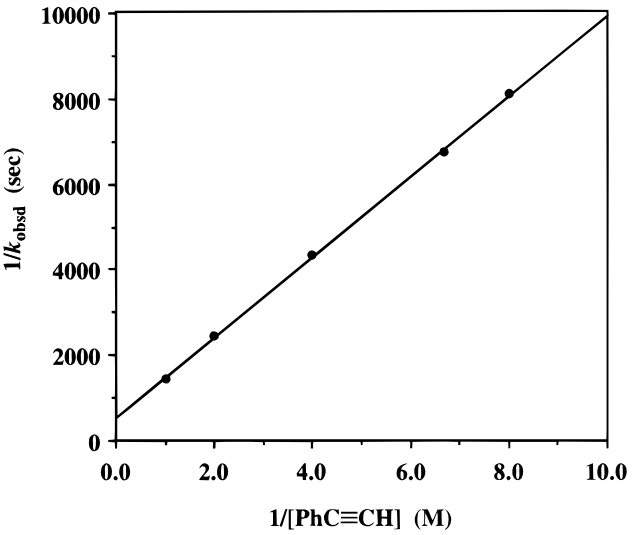

Figure 5. Effect of phenylacetylene concentration on the insertion rate of phenylacetylene into **1b** in CD_2Cl_2 in the presence of added PMe_2Ph at −5 °C. Initial concentration: [**1b**] = 0.025 M; [PMe_2Ph] = 2.5 mM.

In this scheme, steady-state approximation for the concentration of **3b** leads to the following equation:

$$d[\mathbf{3b}]/dt = k_1[\mathbf{1b}] - k_{-1}[PMe_2Ph][\mathbf{3b}] - k_2[PhC{\equiv}CH][\mathbf{3b}] = 0 \quad (2)$$

Thus

$$[\mathbf{3b}] = \frac{k_1[\mathbf{1b}]}{k_{-1}[PMe_2Ph] + k_2[PhC{\equiv}CH]} \quad (3)$$

If the steady state for **3b** holds and the conversion of **4b** to **2b** is a rapid process, the formation rate of **2b** is expressed as

$$d[\mathbf{2b}]/dt = -d[\mathbf{1b}]/dt = k_2[PhC{\equiv}CH][\mathbf{3b}] \quad (4)$$

(17) Kinetic experiments for Figure 5 were conducted in the presence of added PMe_2Ph (2.5 mM) to maintain a constant concentration of free PMe_2Ph in the reaction system. In the kinetic runs at a low concentration of phenylacetylene ([PhC≡CH] = 0.125 and 0.150 M), the effect of change in the acetylene concentration could not be ignored at the later stage of the reaction. Therefore, the rate constants were estimated from the kinetic data at low conversion of **1b** (up to 40.9% conversion at 0.125 M.; up to 51.4% conversion at 0.150 M). The first-order plots exhibited good linear correlations ($r = 1.00$ for 16 data points at 0.125 M.; $r = 0.999$ for 16 data points at 0.150 M).

Scheme 1[a]

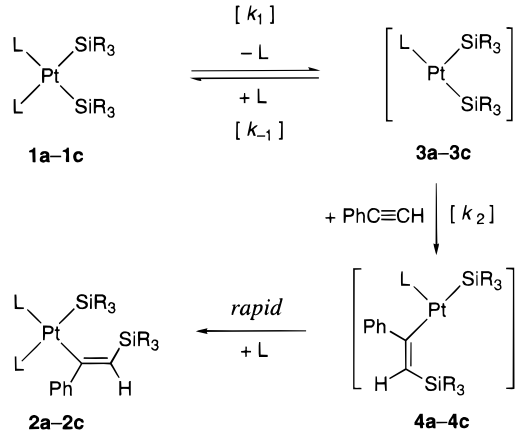

[a] SiR_3 = $SiMe_2Ph$ (a), $SiMePh_2$ (b), $SiPh_3$ (c); L = PMe_2Ph.

Scheme 2[a]

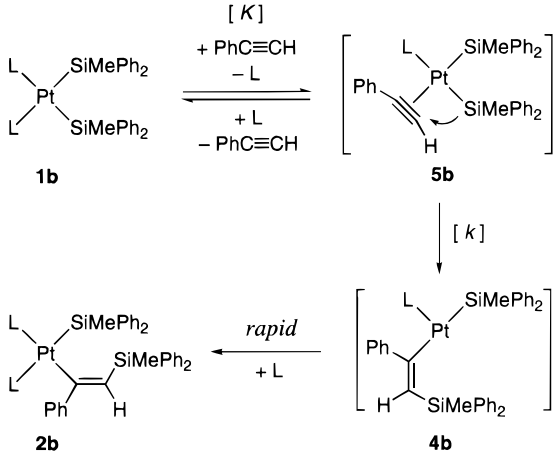

[a] L = PMe_2Ph.

Substitution of eq 3 into eq 4 yields the final rate expression:

$$-\frac{d[\mathbf{1b}]}{dt} = \frac{k_1 k_2[PhC{\equiv}CH]}{k_{-1}[PMe_2Ph] + k_2[PhC{\equiv}CH]}[\mathbf{1b}] \quad (5)$$

Accordingly, the following relation between the k_{obsd} value and the concentration of PMe_2Ph and phenylacetylene can be obtained:

$$\frac{1}{k_{obsd}} = \frac{k_{-1}[PMe_2Ph]}{k_1 k_2[PhC{\equiv}CH]} + \frac{1}{k_1} \quad (6)$$

Equation 6 is fully consistent with the kinetic data. Thus the k_{-1}/k_1k_2 values, which are calculated on the basis of the slopes in Figures 4 and 5, are in good agreement with each other: 3.8×10^5 and 3.76×10^5 s. Furthermore, reciprocals of the intercepts in these figures, which correspond to the rate constant (k_1) for the dissociation of PMe_2Ph ligand from **1b**, are in agreement with each other: 1.9×10^{-3} and 1.8×10^{-3} s^{-1}.

On the other hand, the kinetic relations observed in Figures 4 and 5 also accord with the mechanism in Scheme 2, in which rapid equilibrium between **1b** and **5b** via ligand substitution is presumed prior to the rate-determining insertion of phenylacetylene into the Pt–$SiMePh_2$ bond. The resulting **4b** is rapidly converted to the final product **2b** via the same process as Scheme 1.

In this mechanism, concentration of **5b** at time t is given by the following equation when the equilibration between **1b** and **5b** is rapid enough to keep the equilibrium constant K = [**5b**][PMe_2Ph]/[**1b**][PhC≡CH], irrespective of the reaction progress:

$$[\mathbf{5b}] = \frac{K[PhC{\equiv}CH]}{[PMe_2Ph] + K[PhC{\equiv}CH]}[Pt(SiMePh_2)_2]_{total} \quad (7)$$

where $[Pt(SiMePh_2)_2]_{total}$ = [**1b**] + [**5b**]. Therefore, the formation rate of **2b** is expressed as

$$\frac{d[\mathbf{2b}]}{dt} = -\frac{d}{dt}[Pt(SiMePh_2)_2]_{total} = k[\mathbf{5b}]$$
$$= \frac{kK[PhC{\equiv}CH]}{[PMe_2Ph] + K[PhC{\equiv}CH]}[Pt(SiMePh_2)_2]_{total} \quad (8)$$

The k_{obsd} value is given by the following equation:

$$\frac{1}{k_{obsd}} = \frac{[PMe_2Ph]}{kK[PhC{\equiv}CH]} + \frac{1}{k} \quad (9)$$

On the basis of eq 9 as well as the slopes and intercepts of Figures 4 and 5, the equilibrium constant K in Scheme 2 is estimated as 1.48×10^{-3}; the value corresponds to the [**5b**]/[**1b**] ratio of 0.074–0.592 under the reaction conditions ([PhC≡CH] = 0.125–1.00 M, [PMe_2Ph] = 2.5 mM). Thus, **5b** must be detected by NMR spectroscopy. However, $^{31}P\{^1H\}$ NMR spectra of the reaction solutions exhibited no signals assignable to **5b**, and only the signals of **1b** and **2b** appeared without broadening. Consequently, possibility of the mechanism in Scheme 2 can be excluded.

Complexes **1a** and **1c** showed kinetic behavior very similar to **1b**. Thus, the reaction progress was retarded by addition of free PMe_2Ph to the systems,[18] and the $1/k_{obsd}$ and 1/[PhC≡CH] values were linearly correlated with each other for both systems (r = 0.997 for **1a** and 0.998 for **1c**). Table 3 summarizes the k_1 and k_2/k_{-1} values for the mechanism in Scheme 1, which were estimated from the $1/k_{obsd}$ – 1/[PhC≡CH] plots. The data for **1a** and **1c** were obtained at –5 °C. The reaction of **1b** was too slow to be examined at this temperature and examined at 10 °C.

Table 3. Rate Constants in Scheme 1 for 1a–c[a]

1a (at –5 °C)	$k_1 = 1.46(3) \times 10^{-4}$ s^{-1}	$k_2/k_{-1} = 1.35(9) \times 10^{-2}$
1b (at +10 °C)	$k_1 = 1.8(1) \times 10^{-3}$ s^{-1}	$k_2/k_{-1} = 1.48(9) \times 10^{-3}$
1c (at –5 °C)	$k_1 = 2.8(11) \times 10^{-3}$ s^{-1}	$k_2/k_{-1} = 4.1(13) \times 10^{-4}$

[a] The values were estimated from the $1/k_{obsd}$ – 1/[PhC≡CH] plots, examined in CD_2Cl_2 in the presence of added PMe_2Ph (2.5 mM).

Preparation and Reaction of *cis*-Pt($SiMe_2Ph$)($SiPh_3$)(PMe_2Ph)$_2$ (1f). It has been found that the $SiPh_3$ complex **1c** undergoes the insertion of phenylacetylene more rapidly than the $SiMe_2Ph$ complex **1a**. To examine the reason for the difference between the

(18) The rate constants in the absence and presence of free PMe_2Ph (5.0 mM) are as follows: [**1a**] 1.21×10^{-4} and 0.82×10^{-4} s^{-1}; [**1c**] 1.18×10^{-3} and 1.10×10^{-4} s^{-1} (in CD_2Cl_2, at –5 °C, [PhC≡CH] = 0.50 M).

reaction rates, we next attempted to compare the reactivity of Pt–$SiMe_2Ph$ and Pt–$SiPh_3$ bonds more directly with the unsymmetrical bis(silyl) complex *cis*-$Pt(SiMe_2Ph)(SiPh_3)(PMe_2Ph)_2$ (**1f**).

Reaction of **1c** with $HSiMe_2Ph$ (1 equiv) in benzene at room temperature for 10 min gave a mixture of **1f**, **1c**, and **1a** in a 98.1:1.7:0.2 ratio (eq 10). Recrystallization of the product provided a mixture of **1f** and **1c** in a 97:3 ratio. Several attempts to obtain pure **1f** were unsuccessful. Thus, repeated recrystallizations led to the higher content of **1c**. Elongated reaction time afforded a complex mixture of silylplatinum complexes including *cis*-$PtH(SiPh_3)(PMe_2Ph)_2$. When **1a** was treated with $HSiPh_3$, nearly half of **1a** remained unreacted.

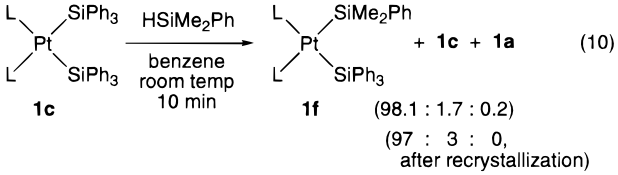

(10)

Treatment of the above mixture of **1f** and **1c** (97:3) with phenylacetylene (10 equiv) in CD_2Cl_2 at room temperature provided four kinds of products **A**–**D** in a 90:4:3:3 **A**:**B**:**C**:**D** ratio (eq 11). Product **D** was **2c** derived from **1c**, as confirmed by $^{31}P\{^1H\}$ NMR spectroscopy. Products **B** and **C** could not be identified due to their low contents. On the other hand, the main product **A** was characterized by NMR spectroscopy as *cis*-Pt{C(Ph)=CH($SiMe_2Ph$)}($SiPh_3$)(PMe_2Ph)$_2$ (**2f**), which is formed by the insertion of phenylacetylene into the Pt–$SiMe_2Ph$ bond of **1f**. Thus, the higher reactivity of Pt–$SiMe_2Ph$ bond than Pt–$SiPh_3$ bond was evidenced.

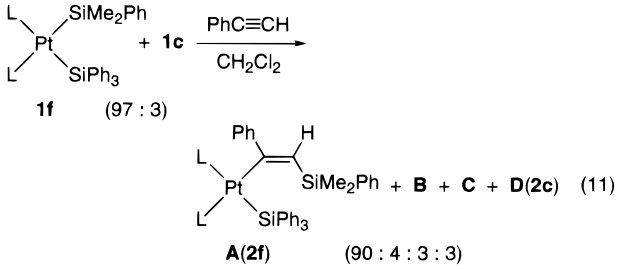

(11)

Discussion

We have found the following reactivity order of bis(silyl)platinum complexes toward the insertion of phenylacetylene: **1c** > **1a** > **1b** ≫ **1d**. The lowest reactivity of **1d** may be attributed to the relatively inert nature of the Pt–$SiFPh_2$ bond, caused by the strongest Pt–Si bond (vide supra). On the other hand, the reactivity order observed for **1a**–**c** (i.e. **1c** > **1a** > **1b**) is apparently inconsistent with the expected order of Pt–Si bond strength. This reason will be discussed in the following section. At the beginning we will analyze the rate constants estimated by kinetic experiments.

As seen from Table 3, the k_2/k_{-1} ratio for **1a** is 33 times as large as that for **1c** at −5 °C, probably because the insertion of phenylacetylene into the Pt–SiR_3 bond (i.e., **3** → **4** in Scheme 1) proceeds more rapidly for **1a** than **1c** (k_2(**1a**) > k_2(**1c**)).[19] The higher reactivity of the Pt–$SiMe_2Ph$ bond than the Pt–$SiPh_3$ bond was also suggested by the reaction of unsymmetrical bis(silyl) complex **1f** (eq 11). These data are in accord with the assumption that the weaker Pt–Si bond possesses the higher reactivity toward insertion. However, even in this situation, **1c** reacts more rapidly with phenylacetylene than **1a**. This is because **1c** undergoes the dissociation of PMe_2Ph more readily than **1a** (compare the k_1 values in Table 3). The k_1 value for **1b** with the least reactivity was 1.8×10^{-3} s^{-1} at 10 °C, which corresponds to the approximate value of 0.9×10^{-4} s^{-1} at −5 °C on the basis of activation parameters. Thus, it is concluded that the reactivity order observed for **1a**–**c** is mainly due to the difference between the dissociation rates of PMe_2Ph.

Chart 1

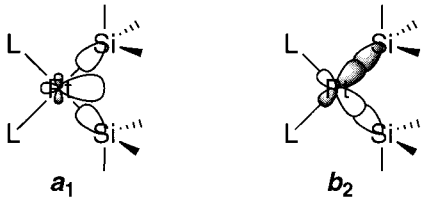

One may expect that the rate of dissociation is affected by bulkiness and the trans influence of silyl ligands; the former facilitates the dissociation by steric congestion around platinum in the order **1a** < **1b** < **1c** and the latter by weakening the Pt–P bonds in the order **1c** < **1b** < **1a**.[20] However, neither factor is correlated with the reactivity order observed (**1c** > **1a** > **1b**). The reason for this disagreement can be seen in the X-ray structures. Thus, it has been found that bis(silyl) complexes have the structures significantly distorted from planarity in the order **1a** < **1c** < **1b** (Table 1). Similarly to *cis*-MR_2L_2 of group 10 metals (R = alkyl, L = tertiary phosphine),[21] the silyl ligands in **1a**–**c** combine with the $Pt(PMe_2Ph)_2$ moiety via two types of bonding orbitals in Chart 1. The a_1 and b_2 symmetry orbitals in this scheme are roughly assigned to donation ($\sigma \rightarrow$ d) and back-donation (d $\rightarrow \sigma^*$) interactions between the combination of two SiR_3 ligands and the platinum center, respectively. Unlike the dialkyl complexes, the present complexes have silyl ligands, which are much more electron-releasing than alkyl ligands. Therefore, the a_1 type orbital interaction can predominate over the b_2 type interaction. In this situation, the bis(silyl) complex has a significantly distorted structure when the distortion is needed to relieve the steric repulsion between the ligands. The higher distortion in **1b** than **1a** can be rationalized in this context, where the sterically more demanding $SiMePh_2$ ligands leads to the more twisted structure.[22] The steric strain inherent in **1b** is effectively relieved by this distortion. In addition,

(19) Since **1a** is less prone to dissociation of the PMe_2Ph ligand than **1c** due to steric reasons (see text), the relative magnitude of the k_{-1} values is considered to be **1a** > **1c**. Accordingly, the relative order k_2(**1a**) > k_2(**1c**) can be estimated from the k_2/k_{-1} values in Table 3.

(20) Sakaki et al. recently reported that the more σ-donating silyl ligand possesses the higher trans influence.[9a]

(21) Albright, T. A.; Burdett, J. K.; Whangbo, M.-H. *Orbital Interactions in Chemistry*; Wiley: New York, 1985. Tatsumi, K.; Hoffmann, R.; Yamamoto, A.; Stille, J. K. *Bull. Chem. Soc. Jpn.* **1981**, *54*, 1857.

(22) Note that the P–Pt–P angle of the most twisted **1b** is significantly wider than that of **1a** and **1c** (Table 1), indicating the least contribution of the b_2 type orbital interaction in **1b**.[21]

the distortion also reduces the direct trans influence of the silyl ligands on the Pt−P bonds. Indeed, **1b** has the shortest Pt−P bonds and the largest $^1J_{Pt-P}$ constant (Table 1). These situations give rise to the stability of **1b** toward the dissociation of PMe_2Ph and reduce the insertion rate.

On the other hand, when the silyl ligand has electron-withdrawing (or less electron-releasing) substituents and possesses an electron-withdrawing character, the b_1 type orbital interaction gains importance, compelling the planarity of the bis(silyl) complex. Complex **1c** should be the case, in which the distortion is modest despite the presence of the most sterically demanding $SiPh_3$ ligands. This situation must provide significant strain energy for **1c**, which will be efficiently released by dissociation of one of the PMe_2Ph ligands. Furthermore, the more planar structure causes the more effective weakening of the Pt−P bonds by silyl ligands with great trans influence; **1c** actually has the longest Pt−P bonds and the smallest $^1J_{Pt-P}$ constant (Table 1). Consequently, **1c** is highly reactive to the dissociation of PMe_2Ph and hence to the insertion of phenylacetylene.

In conclusion, we have found an interesting relation between the reactivities and the structures of bis(silyl)-platinum complexes. The reactivity toward the insertion of phenylacetylene is mainly dictated by the ease of dissociation of the PMe_2Ph ligand. The dissociation rates exhibit rather intricate dependence on the sorts of silyl ligands because the bis(silyl) complexes have distorted structures and the distortion is highly sensitive to the steric and electronic nature of the silyl ligands.

Experimental Section

General Procedure. All manipulations were carried out under a nitrogen atmosphere using conventional Schlenk techniques. Nitrogen gas was dried by passing through P_2O_5 (Merck, SICAPENT). NMR spectra were recorded on a JEOL JNM-A400 or Varian Mercury 300 spectrometer. Chemical shifts are reported in δ (ppm) referred to an internal $SiMe_4$ standard for ^1H and ^{13}C NMR and to an external 85% H_3PO_4 standard for ^{31}P NMR. GLC analysis was performed with a GL Sciences GC-353 instrument equipped with a FID detector and a capillary column (TC-1, 30 m). GC-mass analyses were conducted with a Shimadzu QP-5000 GC-mass spectrometer (EI, 70 eV). THF, Et_2O, and benzene were dried over sodium benzophenone ketyl and distilled prior to use. CH_2Cl_2 was dried over CaH_2 and distilled prior to use. CD_2Cl_2 was dried over $LiAlH_4$, vacuum transferred, and stored under a nitrogen atmosphere.

Preparation of *cis*-Pt(SiMe$_2$Ph)$_2$(PMe$_2$Ph)$_2$ (1a). To a suspension of *cis*-$PtCl_2(PMe_2Ph)_2$ (2.61 g, 4.81 mmol) in THF (25 mL) was added a solution of $PhMe_2SiLi$ in THF (1.17 M, 9.1 mL, 10.6 mmol) at room temperature by means of a syringe. The mixture was stirred at room temperature for 30 min. Methanol (0.1 mL) was added, and the solution was concentrated to dryness. The residue was extracted with benzene (50 mL × 3) and filtered through a filter-paper-tipped cannula. The combined extracts were concentrated to dryness to give a yellow solid of **1a**, which was washed with Et_2O (3 mL × 2) at room temperature and dried under vacuum (1.98 g, 55%). This product was analytically pure. The crystalline product could be obtained by recrystallization from CH_2Cl_2/Et_2O. ^1H NMR (CD_2Cl_2, 23 °C): δ 0.51 (s, $^3J_{Pt-H}$ = 26.8 Hz, 12H, $SiCH_3$), 0.74 (d, $^2J_{P-H}$ = 7.3 Hz, $^3J_{Pt-H}$ = 16.6 Hz, 12H, PCH_3), 7.12−7.18 (m, 2H, Ph), 7.20−7.37 (m, 14H, Ph), 7.63 (dd, 4H, Ph). $^{13}C\{^1H\}$ NMR (CD_2Cl_2, 23 °C): δ 6.8 (t, $^3J_{P-C}$ = 8 Hz, $^2J_{Pt-C}$ = 74 Hz, $SiCH_3$), 15.7 (dd, $^1J_{P-C}$ = 23 Hz, $^3J_{P-C}$ = 12 Hz, $^2J_{Pt-C}$ = 23 Hz, PCH_3), 126.8 (s, Ph), 127.2 (s, Ph), 128.2 (s, Ph), 129.2 (s, Ph), 130.4 (s, Ph), 134.6 (d, $^2J_{P-C}$ = 10 Hz, Ph), 141.2 (m, Ph), 152.7 (m, Ph). $^{31}P\{^1H\}$ NMR (CD_2Cl_2, −70 °C): δ −6.4 (s, $^1J_{Pt-P}$ = 1542 Hz, $^2J_{Si-P(transoid)}$ = 154 Hz, $^2J_{Si-P(cisoid)}$ = 19 Hz, $^2J_{P-P}$ = 23 Hz). Anal. Calcd for $C_{32}H_{44}Si_2P_2Pt$: C, 51.81; H, 5.98. Found: C, 51.95; H, 5.98.

Complex **1b** was prepared according to literature.[10] The ^1H and $^{13}C\{^1H\}$ NMR data hitherto unpublished are as follows. ^1H NMR (CD_2Cl_2): δ 0.42 (s, $^3J_{Pt-H}$ = 30.3 Hz, 6H, $SiCH_3$), 0.55 (d, $^2J_{P-H}$ = 8.3 Hz, $^3J_{Pt-H}$ = 12.2 Hz, 12H, PCH_3), 7.18−7.44 (m, 22H, Ph), 7.73 (dd, 8H, Ph). $^{13}C\{^1H\}$ NMR (CD_2Cl_2): δ 6.4 (s, $^2J_{Pt-C}$ = 88 Hz, $SiCH_3$), 15.6 (d, $^1J_{P-C}$ = 25 Hz, $^2J_{Pt-C}$ = 25 Hz, PCH_3), 127.2 (s, Ph), 127.4 (s, Ph), 128.5 (t, Ph), 129.5 (s, Ph), 130.5 (t, Ph), 136.5 (s, $^3J_{Pt-C}$ = 20 Hz, Ph), 140.8 (m, Ph), 148.5 (m, Ph). The $^{31}P\{^1H\}$ NMR data are reported in ref 11a.

Preparation of *cis*-Pt(SiPh$_3$)$_2$(PMe$_2$Ph)$_2$ (1c). To a solution of *trans*-$PtCl(SiPh_3)(PMe_2Ph)_2$[10a] (1.20 g, 1.57 mmol) in THF (10 mL) was added a THF solution of Ph_3SiLi (0.34 M, 5.8 mL, 1.97 mmol) at room temperature. The mixture was stirred at room temperature for 30 min. Methanol (0.1 mL) was added, and the solution was concentrated to dryness by pumping. The resulting solid was extracted with benzene (5 mL × 3) and filtered through a filter-paper-tipped cannula. The combined extracts were concentrated to dryness to give a yellow solid of **1c**, which was washed with Et_2O (3 mL × 2) at room temperature and dried under vacuum (1.44 g, 93%). This product was spectroscopically pure. The analytically pure complex was obtained by recrystallization from CH_2Cl_2/Et_2O (63%). ^1H NMR (CD_2Cl_2, 23 °C): δ 0.52 (d, $^2J_{P-H}$ = 7.8 Hz, $^3J_{Pt-H}$ = 11.5 Hz, 12H, PCH_3), 7.04−7.14 (m, 18H, Ph), 7.37−7.50 (m, 10H, Ph), 7.65 (dd, 12H, Ph). $^{13}C\{^1H\}$ NMR (CD_2Cl_2, 23 °C): δ 16.0 (s, PCH_3), 126.7 (s, Ph), 127.3 (s, Ph), 128.8 (s, Ph), 129.8 (s, Ph), 130.7 (s, Ph), 137.9 (s, Ph), 140.2 (m, Ph), 144.9 (s, $^2J_{Pt-C}$ = 48 Hz, Ph). $^{31}P\{^1H\}$ NMR (CD_2Cl_2, −70 °C): δ −9.7 (s, $^1J_{Pt-P}$ = 1536 Hz, $^2J_{Si-P(transoid)}$ = 159 Hz, $^2J_{Si-P(cisoid)}$ = 19 Hz, $^2J_{P-P}$ = 23 Hz). Anal. Calcd for $C_{52}H_{52}Si_2P_2Pt$: C, 63.08; H, 5.29. Found: C, 62.59; H, 5.28.

Preparation of *cis*-Pt(SiFPh$_2$)$_2$(PMe$_2$Ph)$_2$ (1d). To a solution of *cis*-$PtMe(SiPh_3)(PMe_2Ph)_2$[6] (230 mg, 0.31 mmol) in benzene (10 mL) was added $HSiFPh_2$ (623 mg, 3.08 mmol) at room temperature. The mixture was stirred at 60 °C for 12 h and then concentrated to dryness, giving a white solid, which was washed with hexane (3 mL × 3) at room temperature and dried under vacuum (230 mg, 85%). The crude product was dissolved in CH_2Cl_2 (ca. 1 mL), Et_2O (ca. 3 mL) was carefully layered, and the solvent layers were allowed to stand at room temperature for 12 h and then at −20 °C for 1 day to give white crystals of **1d** (195 mg, 72%). ^1H NMR (CD_2Cl_2, 23 °C): δ 1.04 (d, $^2J_{P-H}$ = 7.8 Hz, $^3J_{Pt-H}$ = 18.5 Hz, 12H, PCH_3), 7.17−7.31 (m, 16H, Ph), 7.32−7.40 (m, 6H, Ph), 7.61 (dd, 8H, Ph). $^{13}C\{^1H\}$ NMR (CD_2Cl_2, 23 °C): δ 16.5 (d, $^1J_{P-C}$ = 30 Hz, $^2J_{Pt-C}$ = 26 Hz, PCH_3), 124.7 (s, Ph), 128.5 (s, Ph), 128.7 (t, Ph), 130.0 (s, Ph), 130.7 (t, Ph), 135.7 (s, Ph), 139.1 (m, PPh), 144.9(m, Ph). $^{31}P\{^1H\}$ NMR (CD_2Cl_2, 23 °C): δ −4.3 (t, $^1J_{Pt-P}$ = 1522 Hz, $^2J_{Si-P}$ = 76 Hz, $^3J_{F-P}$ = 35 Hz). Anal. Calcd for $C_{40}H_{42}F_2Si_2P_2Pt$: C, 54.97; H, 4.94. Found: C, 54.73; H, 4.64.

Preparation of *cis*-Pt{C(Ph)═CH(SiMe$_2$Ph)}(SiMe$_2$Ph)-(PMe$_2$Ph)$_2$ (2a). While the insertion of phenylacetylene into **1a** proceeded quantitatively with 1 equiv of the acetylene in NMR scale, the following experiment in preparative scale was conducted with a slightly excess amount (1.5 equiv) of phenylacetylene. To a solution of *cis*-$Pt(SiMe_2Ph)_2(PMe_2Ph)_2$ (**1a**, 529 mg, 0.71 mmol) in CH_2Cl_2 (9 mL) was added phenylacetylene (117 μL, 1.07 mmol) at 0 °C. The mixture was stirred at room temperature for 15 min and then concentrated to dryness. The resulting solid of **2a** was washed with a mixture of Et_2O and MeOH (1:10) (5 mL × 3) at −78 °C and dried under vacuum (352 mg, 58%). ^1H NMR (CD_2Cl_2, −20 °C): δ 0.05 (s, $^3J_{Pt-H}$ = 24.8 Hz, 3H, $PtSiCH_3$), 0.43 (s, $^3J_{Pt-H}$ = 22.8 Hz, 3H,

PtSiCH$_3$), 0.60 (s, 3H, PtC=CSiCH$_3$), 0.81 (s, 3H, PtC=CSiCH$_3$), 0.89 (d, $^2J_{P-H}$ = 8.0 Hz, $^3J_{Pt-H}$ = 23.2 Hz, 3H, PCH$_3$), 0.96 (d, $^2J_{P-H}$ = 8.0 Hz, $^3J_{Pt-H}$ = 19.2 Hz, 3H, PCH$_3$), 1.01 (d, $^2J_{P-H}$ = 8.0 Hz, $^3J_{Pt-H}$ = 14.4 Hz, 3H, PCH$_3$), 1.20 (d, $^2J_{P-H}$ = 8.0 Hz, $^3J_{Pt-H}$ = 22.4 Hz, 3H, PCH$_3$), 6.89 (t, 2H, Ph), 7.0−7.4 (m, 17H, Ph), 7.55 (dd, $^4J_{P-H}$ = 18.4 and 4.4 Hz, $^3J_{Pt-H}$ = 134.3 Hz, 1H, PtC=CH), 7.60−7.75 (m, 4H, Ph), 8.00 (d, 2H, Ph). ^{13}C{^{1}H} NMR (CD_2Cl_2, −20 °C): δ 0.3 (s, PtC=CSi*C*H$_3$), 0.9 (s, PtC=CSi*C*H$_3$), 4.7 (d, $^3J_{P-C}$ = 8 Hz, $^2J_{Pt-C}$ = 63 Hz, PtSiCH$_3$), 6.2 (s, $^2J_{Pt-C}$ = 69 Hz, PtSiCH$_3$), 12.5 (d, $^1J_{P-C}$ = 23 Hz, $^2J_{Pt-C}$ = 16 Hz, PCH$_3$), 14.3 (d, $^1J_{P-C}$ = 26 Hz, $^2J_{Pt-C}$ = 27 Hz, PCH$_3$), 16.1 (dd, $^1J_{P-C}$ = 28 Hz, $^3J_{P-C}$ = 5 Hz, $^2J_{Pt-C}$ = 30 Hz, PCH$_3$), 16.7 (dd, $^1J_{P-C}$ = 31 Hz, $^3J_{P-C}$ = 5 Hz, $^2J_{Pt-C}$ = 30 Hz, PCH$_3$), 125.9 (s, PtC=*C*H), 126.9 (s, Ph), 127.0 (s, Ph), 127.1 (s, Ph), 127.4 (s, Ph), 127.6 (s, Ph), 128.1 (s, Ph), 128.2 (s, Ph), 128.3 (s, Ph), 129.1 (s, Ph), 129.3 (s, Ph), 129.5 (s, $^3J_{Pt-C}$ = 46 Hz, Ph), 130.3 (d, $^2J_{P-C}$ = 10 Hz, PPh), 130.4 (d, $^2J_{P-C}$ = 10 Hz, PPh), 134.0 (s, Ph), 134.8 (s, $^3J_{Pt-C}$ = 21 Hz, Ph), 137.7 (d, $^1J_{P-C}$ = 30 Hz, PPh), 138.6 (dd, $^1J_{P-C}$ = 41 Hz, $^3J_{P-C}$ = 5 Hz, PPh), 142.5 (s, PtC=CSi*P*h), 150.9 (dd, $^3J_{P-C}$ = 8 and 5 Hz, $^2J_{Pt-C}$ = 58 Hz, PtSiPh), 152.9 (d, $^3J_{P-C}$ = 5 Hz, $^2J_{Pt-C}$ = 40 Hz, PtC(*P*h)=C), 181.5 (dd, $^2J_{P-C}$ = 99 and 15 Hz, Pt*C*=CH). ^{31}P{^{1}H} NMR (CD_2Cl_2, −20 °C): δ −12.2 (d, $^2J_{P-P}$ = 19 Hz, $^1J_{Pt-P}$ = 1210 Hz, $^2J_{Si-P}$ = 167 Hz), −15.2 (d, $^2J_{P-P}$ = 19 Hz, $^1J_{Pt-P}$ = 1885 Hz). Anal. Calcd for $C_{40}H_{50}Si_2P_2Pt$: C, 56.92; H, 5.97. Found: C, 56.68; H, 5.78.

Preparation of *cis*-Pt{C(Ph)=CH(SiMePh$_2$)}(SiMePh$_2$)(PMe$_2$Ph)$_2$ (2b) and *cis*-Pt{C(Ph)=CH(SiPh$_3$)}(SiPh$_3$)(PMe$_2$Ph)$_2$ (2c). The title compounds were prepared similarly to **2a** using **1b** or **1c** in place of **1a** and isolated as white solids in 76 (**2b**) and 83% (**2c**) yields.

Compound **2b**. ^{1}H NMR (CD_2Cl_2, −20 °C): δ 0.53 (d, $^4J_{P-P}$ = 2.0 Hz, $^3J_{Pt-H}$ = 24.4 Hz, 3H, PtSiCH$_3$), 0.72 (d, $^2J_{P-H}$ = 7.2 Hz, $^3J_{Pt-H}$ = 15.2 Hz, 3H, PCH$_3$), 0.87 (d, $^2J_{P-H}$ = 7.6 Hz, $^3J_{Pt-H}$ = 19.0 Hz, 3H, PCH$_3$), 1.01 (d, $^2J_{P-H}$ = 8.4 Hz, $^3J_{Pt-H}$ = 17.2 Hz, 3H, PCH$_3$), 1.13 (d, $^2J_{P-H}$ = 7.6 Hz, $^3J_{Pt-H}$ = 19.6 Hz, 3H, PCH$_3$), 1.43 (s, 3H, PtC=CSiCH$_3$), 6.75 (t, 2H, Ph), 6.85−7.45 (m, 16H, Ph), 7.55−7.80 (m, 9H, Ph), 7.80 (dd, $^4J_{P-H}$ = 18.8 and 3.6 Hz, $^3J_{Pt-H}$ = 130.3 Hz, 1H, PtC=CH). ^{13}C{^{1}H} NMR (CD_2Cl_2, −20 °C): δ −1.5 (s, $^1J_{Si-C}$ = 53 Hz, PtC=CSi*C*H$_3$), 4.0 (d, $^3J_{P-C}$ = 5 Hz, $^2J_{Pt-C}$ = 63 Hz, PtSiCH$_3$), 12.1 (d, $^1J_{P-C}$ = 23 Hz, PCH$_3$), 14.6 (d, $^1J_{P-C}$ = 28 Hz, $^3J_{P-C}$ = 3 Hz, $^2J_{Pt-C}$ = 29 Hz, PCH$_3$), 15.4 (d, $^1J_{P-C}$ = 30 Hz, $^2J_{Pt-C}$ = 28 Hz, PCH$_3$), 17.0 (d, $^1J_{P-C}$ = 30 Hz, $^3J_{P-C}$ = 4 Hz, $^2J_{Pt-C}$ = 35 Hz, PCH$_3$), 123.2 (t, $^2J_{Pt-C}$ = 56.2 Hz PtC=*C*H), 125.8 (s, Ph), 126.9 (s, Ph), 127.0 (s, Ph), 127.1 (s, Ph), 127.7 (s, Ph), 127.8 (s, Ph), 128.1 (t, Ph), 128.5 (s, Ph), 129.0 (s, Ph), 129.1 (s, $^3J_{Pt-C}$ = 46 Hz, Ph), 130.4 (d, $^2J_{P-C}$ = 10 Hz, PPh), 130.5 (d, $^2J_{P-C}$ = 10 Hz, PPh), 134.4 (s, SiPh), 134.6 (s, SiPh), 135.8 (s, SiPh), 135.9 (s, $^3J_{Pt-C}$ = 23 Hz, Ph), 137.5 (d, $^1J_{P-C}$ = 31 Hz, PPh), 138.4 (dd, $^1J_{P-C}$ = 41 Hz, $^3J_{P-C}$ = 5 Hz, PPh), 140.5 (s, SiPh), 141.1 (s, SiPh), 146.5 (d, $^3J_{P-C}$ = 3 Hz, $^2J_{Pt-C}$ = 60 Hz, SiPh), 147.2 (dd, $^3J_{P-C}$ = 8 and 3 Hz, SiPh), 152.3 (d, $^3J_{P-C}$ = 5 Hz, $^2J_{Pt-C}$ = 36 Hz, PtC(*P*h)=C), 182.6 (dd, $^2J_{P-C}$ = 97 and 15 Hz, $^1J_{Pt-C}$ = 759 Hz, Pt*C*=CH). ^{31}P{^{1}H} NMR (CD_2Cl_2, −20 °C): δ −13.1 (d, $^2J_{P-P}$ = 18 Hz, $^1J_{Pt-P}$ = 1261 Hz, $^2J_{Si-P}$ = 170 Hz), −17.4 (d, $^2J_{P-P}$ = 18 Hz, $^1J_{Pt-P}$ = 1853 Hz). Anal. Calcd for $C_{50}H_{54}Si_2P_2Pt$: C, 62.03; H, 5.62. Found: C, 61.68; H, 5.45.

Compound **2c**. ^{1}H NMR (CD_2Cl_2, −20 °C): δ 0.55 (d, $^2J_{P-H}$ = 8.3 Hz, $^3J_{Pt-H}$ = 18.5 Hz, 3H, PCH$_3$), 0.92 (d, $^2J_{P-H}$ = 8.3 Hz, $^3J_{Pt-H}$ = 18.1 Hz, 3H, PCH$_3$), 1.03 (d, $^2J_{P-H}$ = 7.8 Hz, $^3J_{Pt-H}$ = 15.6 Hz, 3H, PCH$_3$), 1.13 (d, $^2J_{P-H}$ = 8.3 Hz, $^3J_{Pt-H}$ = 17.1 Hz, 3H, PCH$_3$), 6.53 (t, 2H, Ph), 6.85−7.50 (m, 31H, Ph), 7.56 (d, 6H, Ph), 7.66 (dd, $^3J_{Pt-H}$ = 130.8 Hz, $^4J_{P-H}$ = 3.9 Hz, $^4J_{P-H}$ = 19.5 Hz, 1H, PtC=CH). ^{13}C{^{1}H} NMR (CD_2Cl_2, −20 °C): δ 13.7 (d, $^1J_{P-C}$ = 25 Hz, $^2J_{Pt-C}$ = 23 Hz, PCH$_3$), 14.5 (d, $^1J_{P-C}$ = 26 Hz, $^2J_{Pt-C}$ = 29 Hz, PCH$_3$), 16.5 (d, $^1J_{P-C}$ = 33 Hz, $^2J_{Pt-C}$ = 33 Hz, PCH$_3$), 16.8 (d, $^1J_{P-C}$ = 31 Hz, $^2J_{Pt-C}$ = 33 Hz, PCH$_3$), 125.8 (s, PtC=*C*H), 126.0−127.0 (m, Ph), 127−128 (m, Ph), 128.2 (t, Ph), 128.9 (s, Ph), 129.1 (s, Ph), 129.6 (s, $^3J_{Pt-C}$ = 40 Hz, Ph), 130.0 (s, Ph), 130.4 (d, $^2J_{P-C}$ = 8 Hz, PPh), 131.3 (d, $^2J_{P-C}$ = 10 Hz, PPh), 136.0 (d, $^1J_{P-C}$ = 16 Hz, PPh), 136.3−138.2 (m, Ph), 144.7 (s, $^2J_{Pt-C}$ = 50 Hz, SiPh), 154.1 (d, $^2J_{Pt-C}$ = 33 Hz, PtC(*P*h)=C), 182.9 (dd, $^1J_{Pt-C}$ = 770 Hz, $^2J_{P-C}$ = 100 and 16 Hz, Pt*C*=CH). ^{31}P{^{1}H} NMR (CD_2Cl_2, −20 °C): δ −14.4 (d, $^2J_{P-P}$ = 20 Hz, $^1J_{Pt-P}$ = 1246 Hz, $^2J_{Si-P}$ = 174 Hz), −17.9 (d, $^2J_{P-P}$ = 20 Hz, $^1J_{Pt-P}$ = 1820 Hz). Anal. Calcd for $C_{60}H_{58}Si_2P_2Pt$: C, 65.97; H, 5.35. Found: C, 65.88; H, 5.20.

Preparation of *cis*-Pt{C(Ph)=CH(SiFPh$_2$)}(SiFPh$_2$)(PMe$_2$Ph)$_2$ (2d). To a solution of *cis*-Pt(SiFPh$_2$)$_2$(PMe$_2$Ph)$_2$ (230 mg, 0.26 mmol) in C_6H_6 (5 mL) was added phenylacetylene (145 μL, 1.32 mmol) at room temperature. The mixture was stirred at 60 °C for 10 min and concentrated to dryness to give a white solid of **2d**, which was washed with hexane (3 mL × 3) at room temperature and dried under vacuum (242 mg, 94%). ^{1}H NMR (CD_2Cl_2, −20 °C): δ 0.58 (d, $^2J_{P-H}$ = 7.6 Hz, $^3J_{Pt-H}$ = 16.0 Hz, 3H, PCH$_3$), 0.98 (d, $^2J_{P-H}$ = 8.8 Hz, $^3J_{Pt-H}$ = 17.6 Hz, 3H, PCH$_3$), 1.09 (d, $^2J_{P-H}$ = 8.4 Hz, $^3J_{Pt-H}$ = 21.6 Hz, 3H, PCH$_3$), 1.32 (d, $^2J_{P-H}$ = 8.8 Hz, $^3J_{Pt-H}$ = 23.2 Hz, 3H, PCH$_3$), 6.86−7.00 (m, 4H, Ph), 7.04−7.46 (m, 25H, Ph, PtC=CH), 7.54 (dd, Ph), 7.67−7.82 (m, 4H, Ph). ^{13}C{^{1}H} NMR (CD_2Cl_2, −20 °C): δ 11.9 (dd, $^1J_{P-C}$ = 25 Hz, $^4J_{F-C}$ = 13 Hz, PCH$_3$), 13.8 (dd, $^1J_{P-C}$ = 28 Hz, $^4J_{F-C}$ = 15 Hz, PCH$_3$), 16.1 (dd, $^1J_{P-C}$ = 31 Hz, $^4J_{F-C}$ = 16 Hz, PCH$_3$), 14.9 (m, PCH$_3$), 120.7 (m, PtC=*C*H), 126.5 (s, Ph), 126.8 (s, Ph), 127.0 (s, Ph), 127.3 (s, Ph), 127.6 (s, Ph), 127.9 (s, Ph), 128.0 (s, Ph), 128.2 (s, Ph), 128.3 (s, Ph), 129.3 (s, Ph), 129.4 (s, Ph), 129.5 (s, Ph), 129.6 (s, Ph), 129.9 (s, Ph), 130.6 (s, Ph), 130.6 (s, Ph), 134.2 (d, $^2J_{P-C}$ = 12 Hz, PPh), 134.5 (s, Ph), 134.8 (s, Ph), 135.1 (d, $^2J_{P-C}$ = 30 Hz, PPh), 136.6 (d, $^1J_{P-C}$ = 69 Hz, PPh), 136.7 (d, $^1J_{P-C}$ = 69 Hz, PPh), 136.9 (d, $^1J_{P-C}$ = 48 Hz, PPh), 137.4 (d, $^1J_{P-C}$ = 43 Hz, PPh), 144.9 (m, PtC=CSi*P*h), 146.1 (t, $^2J_{Pt-C}$ = 102 Hz, PtSiPh), 151.4 (d, $^3J_{P-C}$ = 3 Hz, $^2J_{Pt-C}$ = 40 Hz, PtC(*P*h)=C), 188.6 (dd, $^2J_{P-C}$ = 94 and 15 Hz, $^1J_{Pt-C}$ = 750 Hz, Pt*C*=CH). ^{31}P{^{1}H} NMR (CD_2Cl_2, −20 °C): δ −9.2 (dd, $^2J_{P-P}$ = 22 Hz, $^3J_{F-P}$ = 43 Hz, $^1J_{Pt-P}$ = 1337 Hz, $^2J_{Si-P}$ = 199 Hz), −13.2 (dd, $^2J_{P-P}$ = 22 Hz, $^3J_{F-P}$ = 9 Hz, $^1J_{Pt-P}$ = 1819 Hz). Anal. Calcd for $C_{48}H_{48}F_2Si_2P_2Pt$: C, 59.06; H, 4.96. Found: C, 58.69; H, 4.78.

Preparation of *cis*-Pt(CH=CHSiPh$_3$)(SiPh$_3$)(PMe$_2$Ph)$_2$ (2e). Complex **1c** (376 mg, 0.38 mmol) was placed in a 50 mL Schlenk tube and dissolved in CH_2Cl_2 (1.5 mL) at room temperature. The system was evacuated and acetylene gas (1 atm) was introduced at 0 °C. The solution was stirred at room temperature for 15 min and concentrated to dryness by pumping to give a white solid of **2e**, which was washed with Et_2O (3 mL × 3) at −78 °C and dried under vacuum (332 mg, 86%). ^{1}H NMR (CD_2Cl_2, 0 °C): δ 0.65 (d, $^2J_{P-H}$ = 8.3 Hz, $^3J_{Pt-H}$ = 18.5 Hz, 3H, PCH$_3$), 0.81 (d, $^2J_{P-H}$ = 7.8 Hz, $^3J_{Pt-H}$ = 14.6 Hz, 3H, PCH$_3$), 1.05 (d, $^2J_{P-H}$ = 7.8 Hz, $^3J_{Pt-H}$ = 18.3 Hz, 3H, PCH$_3$), 1.34 (d, $^2J_{P-H}$ = 8.3 Hz, $^3J_{Pt-H}$ = 18.1 Hz, 3H, PCH$_3$), 6.84 (m, 2H, Ph), 6.96−7.44 (m, 27H, Ph, PtC=CH), 7.49 (dd, 6H, Ph), 7.58 (dd, Ph), 9.20 (ddd, $^3J_{H-H}$ = 5.4 Hz, $^3J_{P-H}$ = 17.6 and 2.4 Hz, PtCH=C). ^{13}C{^{1}H} NMR (CD_2Cl_2, 0 °C): δ 12.3 (d, $^1J_{P-C}$ = 20 Hz, PCH$_3$), 15.8 (dd, $^1J_{P-C}$ = 30 Hz, $^3J_{P-C}$ = 3 Hz, $^2J_{Pt-C}$ = 30 Hz, PCH$_3$), 16.2 (dd, $^1J_{P-C}$ = 30 Hz, $^3J_{P-C}$ = 3 Hz, $^2J_{Pt-C}$ = 30 Hz, PCH$_3$), 17.1 (dd, $^1J_{P-C}$ = 30 Hz, $^3J_{P-C}$ = 3 Hz, $^2J_{Pt-C}$ = 30 Hz, PCH$_3$), 124.0 (m, PtC=*C*H), 126.8 (s, Ph), 127.1 (s, Ph), 127.6 (s, Ph), 128.2 (t, Ph), 128.9 (s, Ph), 129.2 (s, Ph), 129.4 (s, Ph), 130.5 (d, $^2J_{P-C}$ = 12 Hz, PPh), 130.6 (d, $^2J_{P-C}$ = 12 Hz, PPh), 136.7 (s, SiPh), 137.4 (s, $^3J_{Pt-C}$ = 20 Hz, SiPh), 137.7 (s, SiPh), 138.0 (d, $^1J_{P-C}$ = 38 Hz, PPh), 138.8 (dd, $^1J_{P-C}$ = 41 Hz, $^3J_{P-C}$ = 5 Hz, PPh), 144.8 (d, $^3J_{P-C}$ = 3 Hz, $^2J_{Pt-C}$ = 50 Hz, SiPh), 179.0 (dd, $^2J_{P-C}$ = 98 and 15 Hz, $^1J_{Pt-C}$ = 709 Hz, Pt*C*=CH). ^{31}P{^{1}H} NMR (CD_2Cl_2, 0 °C): δ −12.3 (d, $^2J_{P-P}$ = 20 Hz, $^1J_{Pt-P}$ = 1390 Hz, $^2J_{Si-P}$ = 173 Hz), −16.4 (d, $^2J_{P-P}$ = 20 Hz, $^1J_{Pt-P}$ = 1821 Hz). Anal. Calcd for $C_{54}H_{54}Si_2P_2Pt$: C, 63.82; H, 5.36. Found: C, 63.62; H, 5.20.

Reactions of 1c with Ethylene and 1-Hexyne. Ethylene gas was passed into a solution of **1c** (14.0 mg, 0.014 mmol) in CH_2Cl_2 (1 mL) for 5 min at −20 °C. The pale yellow solution was warmed to room temperature and stirred for 7.5 h. GLC

Table 4. Crystal Data and Details of the Structure Determination for 1a, 1c, and 2e

	1a	1c	2e
formula	$C_{32}H_{44}P_2Si_2Pt$	$C_{52}H_{52}P_2Si_2Pt$	$C_{54}H_{54}P_2Si_2Pt$
fw	741.91	990.19	1016.23
cryst size, mm	0.4 × 0.4 × 0.3	0.15 × 0.1 × 0.1	0.45 × 0.4 × 0.3
cryst system	monoclinic	monoclinic	triclinic
space group	*C*2/*c* (No. 15)	$P2_1/n$ (No. 14)	$P\bar{1}$ (No. 2)
a, Å	17.546(2)	11.477(4)	14.124(8)
b, Å	11.398(4)	19.06(1)	14.899(8)
c, Å	17.643(5)	20.943(4)	12.351(2)
α, deg			100.29(3)
β, deg	110.24(2)	96.59(2)	106.99(3)
γ, deg			100.55(4)
V, Å^3	3310(1)	4550(2)	2367(2)
Z	4	4	2
d_{calcd}, g cm^{-3}	1.488	1.445	1.425
μ(Mo Kα), cm^{-1}	44.09	32.28	31.04
2*θ* range, deg	4.0−55.0	4.0−54.9	4.0−45.0
scan type	*ω*−2*θ*	*ω*−2*θ*	*ω*−2*θ*
Δ*ω*, deg	1.31 + 0.30 tan *θ*	1.41 + 0.35 tan *θ*	1.15 + 0.30 tan *θ*
scan speed, deg min^{-1}	16, fixed	16, fixed	8, fixed
temp, K	293	293	293
linear decay, %	4.93	2.66	7.33
abs corr	empirical	empirical	empirical
min and max trans factors	0.717, 1.00	0.839, 1.00	0.588, 1.00
no. of reflcns collcd	4118	8522	6487
no. of unique reflcns	3985 (R_{int} = 0.018)	8285 (R_{int} = 0.057)	6183 (R_{int} = 0.050)
no. of observed reflections	3356 ($I = 3\sigma(I)$)	4538 ($I = 2\sigma(I)$)	5366 ($I = 3\sigma(I)$)
no. of variables	169	515	533
R	0.026	0.042	0.031
R_w	0.035	0.058	0.041
goodness of fit	1.12	0.96	1.10
max Δ/*σ* in final cycle	0.00	0.01	0.00
max and min peak, e Å^{-3}	0.94, −0.99 (near Pt)	1.24, −1.05 (near Pt)	0.96, −1.20 (near Pt)

analysis of the resulting solution using $MeSiPh_3$ as an internal standard revealed the formation of CH_2=$CHSiPh_3$ in 93% yield. The formation of vinylsilane was also confirmed by GC-mass spectrometry.

To a solution of **1c** (103 mg, 0.104 mmol) in CH_2Cl_2 (2 mL) was added 1-hexyne (38 μL, 0.33 mmol) by means of a syringe. The solution was stirred at room temperature for 30 min. The $^{31}P\{^1H\}$ NMR spectrum exhibited two sets of doublets assignable to the insertion complex in 96% selectivity: δ −13.0 (d, $^2J_{P-P}$ = 20 Hz, $^1J_{Pt-P}$ = 1403 Hz), −20.8 (d, $^2J_{P-P}$ = 20 Hz, $^1J_{Pt-P}$ = 1606 Hz). Volatile materials were removed by pumping, and the resulting oily material was washed with pentane (3 mL × 3) at 0 °C and dried under vacuum (72 mg). $^{31}P\{^1H\}$ NMR of the product exhibited many unidentified signals together with the doublets arising from the insertion complex. Further purification by recrystallization was unsuccessful.

X-ray Diffraction Studies. Single crystals for X-ray diffraction study were grown by slow diffusion of a CH_2Cl_2 solution to Et_2O at −20 °C. All measurements were performed on a Rigaku AFC7R (for **1a** and **1c**) or Rigaku AFC7 (for **2e**) four-circle diffractometer with graphite monochromated Mo Kα radiation (λ = 0.710 69 Å). Unit cell dimensions were obtained from a least-squares treatment of the setting angles of automatically centered 25 reflections with θ > 25°. Diffraction data were collected at 20 °C using the *ω*−2*θ* scan technique at a scan rate of 16° (for **1a** and **1c**) or 8° min^{-1} (for **2e**) in *ω*. The data were corrected for Lorentz and polarization effects, decay (based on three standard reflections monitored at every 150 reflection measurements), and absorption (empirical, based on azimuthal scans of three reflections).

All calculations were performed with the TEXSAN Crystal Structure Analysis Package provided by Rigaku Corp. The scattering factors were taken from ref 23. The structures were solved by heavy atom Patterson methods (PATTY) and expanded using Fourier techniques (DIRDIF94). Each structure was refined by full-matrix least-squares with anisotropic thermal parameters for all non-hydrogen atoms. In the final cycles of refinement, hydrogen atoms were located at idealized positions (d(C−H) = 0.95 Å) with isotropic temperature factors ($B_{iso} = 1.20B_{bonded\ atom}$) and were included in the calculation without refinement of their parameters. The function minimized in least-squares was $\sum w(|F_o| - |F_c|)^2$ ($w = 1/[\sigma^2(F_o)]$). Crystal data and details of data collection and refinement are summarized in Table 4. Additional information is available as Supporting Information.

The unit cell dimensions and systematic absences in the diffractometer data of **1a** (*hkl*, $h + k \neq 2n$; *h*0*l*, $l \neq 2n$) suggested the space group *Cc* (No. 9) or *C*2/*c* (No. 15). The structure was initially solved and refined in the higher symmetrical space group *C*2/*c*, and the least-squares calculation successfully converged (maximum Δ/*σ* in the final cycle = 0.00). A trial with alternative space group *Cc* did not converge sufficiently (maximum Δ/*σ* in the final cycle = 1.43). The space group $P2_1/n$ (No. 14) for **1c** was uniquely determined (*h*0*l*, $h + l \neq 2n$; 0*k*0, $k \neq 2n$). The space group for **2e** ($P\bar{1}$ (No. 2)) was based on the unit cell dimensions and statistical analysis of the intensity distribution. The refinement converged sufficiently (maximum Δ/*σ* in the final cycle = 0.00), and thereby the other possibility (*P*1) was not examined.

Kinetic Studies. A typical procedure is as follows. *cis*-Pt(SiMePh$_2$)(PMe$_2$Ph)$_2$ (**1b**) (13.0 mg, 15.0 μmol) was placed in an NMR sample tube equipped with a rubber septum cap and the system was replaced with nitrogen gas at room temperature. Phenylacetylene (32.8 μL, 0.300 mmol) was added, and a 10 mM solution of 4,4′-dimethylbiphenyl in CD_2Cl_2 was added at −50 °C to adjust the total volume of the solution to be 0.6 mL. The sample was placed in an NMR sample probe controlled to −5.0 ± 0.1 °C and examined by ^1H NMR spectroscopy. The time course of the insertion was followed by measuring the relative peak integration of the methyl signal of 4,4′-dimethylbiphenyl (δ 2.38) and the $SiCH_3$ signal of the product **2b** (δ 1.48) at intervals. All kinetic studies were similarly conducted. The reaction of **1a** was followed by $^{31}P\{^1H\}$ NMR spectroscopy.

(23) Cromer, D. T.; Waber, J. T. *International Tables for X-ray Crystallography*; The Kynoch Press: Birmingham, U.K., 1974; Vol. IV.

Preparation and Reaction of *cis*-Pt(SiMe$_2$Ph)(SiPh$_3$)(PMe$_2$Ph)$_2$ (1f). Complex **1c** (150 mg, 0.151 mmol) was placed in a 25 mL Schlenk tube and dissolved in benzene (8 mL). $HSiMe_2Ph$ (20.6 mg, 0.151 mmol) was added. The solution was stirred at room temperature for 10 min and then concentrated to dryness by pumping. The resulting yellow solid was washed with hexane (3 mL × 3) and dissolved in CH_2Cl_2 (ca. 1 mL). Et_2O (ca. 3 mL) was layered, and the solvent layers were allowed to stand at room temperature for 12 h and then at −20 °C for 1 day to give yellow crystals (79 mg). The $^{31}P\{^1H\}$ NMR spectrum (CD_2Cl_2, −50 °C) indicated the presence of **1f** and **1c** in a 97:3 ratio. Several attempts to obtain pure **1f** were unsuccessful.

Compound **1f**. ^1H NMR (CD_2Cl_2): δ −0.06 (s, $^3J_{Pt-H}$ = 24.9 Hz, 6H, $SiCH_3$), 0.60 (d, $^2J_{P-H}$ = 7.8 Hz, $^3J_{Pt-H}$ = 16.6 Hz, 12H, PCH_3), 7.25−7.44 (m, 22H, Ph), 7.66 (dd, 2H, Ph), 7.99 (dd, 6H, Ph). $^{13}C\{^1H\}$ NMR (CD_2Cl_2): δ 5.7 (s, $^2J_{Pt-C}$ = 71 Hz, $SiCH_3$), 15.7 (d, $^1J_{P-C}$ = 25 Hz, $^2J_{Pt-C}$ = 20 Hz, PCH_3), 126.9 (s, SiPh), 127.2 (s, SiPh), 127.3 (s, SiPh), 127.5 (s, SiPh), 128.4 (d, $^3J_{P-C}$ = 8 Hz, PPh), 129.5 (s, PPh), 130.5 (m, PPh), 134.6 (s, $^3J_{Pt-C}$ = 15 Hz, SiPh), 137.6 (s, $^3J_{Pt-C}$ = 22 Hz, SiPh), 140.8 (d, $^1J_{P-C}$ = 43 Hz, PPh), 145.8 (t, $^2J_{Pt-C}$ = 53 Hz, SiPh), 152.5 (t, SiPh). $^{31}P\{^1H\}$ NMR (CD_2Cl_2, −50 °C): δ −6.3 (d, $^2J_{P-P}$ = 23 Hz, $^1J_{Pt-P}$ = 1679 Hz, $^2J_{Si-P}$ = 160 Hz), −9.1 (d, $^2J_{P-P}$ = 25 Hz, $^1J_{Pt-P}$ = 1453 Hz, $^2J_{Si-P}$ = 146 Hz).

The mixture of **1f** and **1c** thus prepared (18.8 mg, 21.7 μmol) was placed in an NMR sample tube equipped with a rubber septum cap and dissolved in CD_2Cl_2 (0.6 mL) at room temperature. Phenylacetylene (23.8 μL, 0.217 mmol) was added, and the solution was examined by $^{31}P\{^1H\}$ NMR spectroscopy at 0 °C, showing the formation of four kinds of products (**A**−**D**) in a 90:4:3:3 ratio: **A** (δ −14.5 (d), −17.5 (d); $^2J_{P-P}$ = 19 Hz), **B** (δ −12.6 (d), −17.0 (d); $^2J_{P-P}$ = 21 Hz), **C** (δ −13.5 (d), −17.0 (d); $^2J_{P-P}$ = 20 Hz), **D** (δ −14.4 (d), −17.9 (d); $^2J_{P-P}$ = 20 Hz). Product **D** was assigned to **2c** by comparison of the NMR data with those of the authentic sample. On the other hand, product **A** was identified as *cis*-Pt{C(Ph)═CH(SiMe$_2$Ph)}(SiPh$_3$)(PMe$_2$Ph)$_2$ (**2f**) on the basis of the following NMR data. The characteristic features for the insertion of phenylacetylene into the Pt−SiMe$_2$Ph bond are the absence of P−H and P−C couplings in the signals arising from the methyl protons and carbons of SiMe$_2$Ph group.

Compound **2f**. ^1H NMR (CD_2Cl_2, −20 °C): δ 0.41 (s, 1H, $SiCH_3$), 0.65 (d, $^2J_{P-H}$ = 8.4 Hz, $^3J_{Pt-H}$ = 19.2 Hz, 3H, PCH_3), 0.88 (s, 3H, $SiCH_3$), 1.03 (d, $^2J_{P-H}$ = 8.1 Hz, 3H, PCH_3), 1.05 (d, $^2J_{P-H}$ = 8.1 Hz, 3H, PCH_3), 1.11 (d, $^2J_{P-H}$ = 8.1 Hz, 3H, PCH_3), 6.86 (t, 2H, Ph), 6.95−7.60 (m, 34H, Ph, PtC═CH). $^{13}C\{^1H\}$ NMR (CD_2Cl_2, −20 °C): δ 0.3 (s, $SiCH_3$), 0.5 (s, $SiCH_3$), 13.0 (d, $^1J_{P-C}$ = 24 Hz, $^2J_{Pt-C}$ = 18 Hz, PCH_3), 14.4 (dd, $^1J_{P-C}$ = 29 Hz, $^3J_{P-C}$ = 3 Hz, PCH_3), 15.5 (dd, $^1J_{P-C}$ = 31 Hz, $^3J_{P-C}$ = 4 Hz, PCH_3), 17.1 (dd, $^1J_{P-C}$ = 31 Hz, $^3J_{P-C}$ = 4 Hz, PCH_3), 125.4 (s, PtC═*C*H), 126.2 (s, Ph), 126.5 (s, Ph), 126.9 (s, Ph), 127.6 (s, Ph), 128.1 (s, Ph), 128.2 (d, $^3J_{P-C}$ = 7 Hz, PPh), 128.4 (d, $^3J_{P-C}$ = 9 Hz, PPh), 129.2 (s, $^3J_{Pt-C}$ = 44 Hz, PtC(*Ph*)═CH), 129.9 (s, Ph), 130.4 (d, $^2J_{P-C}$ = 10 Hz, PPh), 131.0 (d, $^2J_{P-C}$ = 11 Hz, PPh), 133.9 (s, Ph), 137.1−138.5 (m, Ph), 144.2 (s, PtC═CSi*Ph*), 144.6 (d, $^3J_{P-C}$ = 8 Hz, $^2J_{Pt-C}$ = 53 Hz, PtSi*Ph*), 152.5 (d, $^3J_{P-C}$ = 5 Hz, $^2J_{Pt-C}$ = 33 Hz, PtC(*Ph*)═CH), 178.5 (dd, $^2J_{P-C}$ = 97 and 14 Hz, $^1J_{Pt-C}$ = 756 Hz, Pt*C*═CH). $^{31}P\{^1H\}$ NMR (CD_2Cl_2, −20 °C): δ −14.5 (d, $^2J_{P-P}$ = 19 Hz, $^1J_{Pt-P}$ = 1275 Hz, $^2J_{Si-P}$ = 175 Hz), −13.2 (d, $^2J_{P-P}$ = 20 Hz, $^1J_{Pt-P}$ = 1803 Hz).

Acknowledgment. We are indebted to Prof. S. Sakaki (Kumamoto University) for helpful discussions and comments. This work was supported by a Grant-in-Aid for Scientific Research on Priority Area "The Chemistry of Inter-element Linkage" (Grant No. 09239105) from the Ministry of Education, Science, Sports and Culture, Japan.

Supporting Information Available: Details of the structure determination of **1a**, **1c**, and **2e** including figures giving atomic numbering schemes and tables of atomic coordinates, thermal parameters, and full bond distances and angles (23 pages). Ordering information is given on any current masthead page.

OM980610W